Heating Effect of Dielectric Barrier Discharges for Direct Medical Treatment

Halim Ayan, Gregory Fridman, David Staack, Alexander F. Gutsol, Victor N. Vasilets, Alexander A. Fridman, and Gary Friedman

***Abstract*—Several variations of dielectric barrier discharge (DBD) have been developed for nondamaging living-tissue sterilization and blood coagulation. This so-called floating electrode DBD (FE-DBD) has been shown by histology to not damage the treated tissue. Nevertheless, preliminary experiments show that a person who touches the FE-DBD can feel the discharge action. Some of these unpleasant sensations are related to the thermal effects of the plasma. These thermal effects and other important parameters of the discharge are strongly dependent on the electrical properties of the discharge, i.e., driving voltage and waveform shape. In this paper, we first employed sinusoidal driving waveform for medical applications. After that, in order to increase the uniformity and decrease the temperature, we employed a microsecond-pulsed waveform system with a few microsecond pulse durations. Both plasma systems have been analyzed and compared for thermal effects and temperature of the discharge in order to determine the possibilities to control the heating effect with driving waveform.**

***Index Terms*—Atmospheric pressure discharges, dielectric barrier discharges (DBDs), nonthermal plasma, plasma medicine.**

I. Background and Introduction

In recent years, nonthermal atmospheric pressure plasmas have attracted researchers from a wide variety of fields due to the many potential applications. Dielectric barrier discharges (DBDs) are significant among all types of nonthermal plasmas because of their ease of operation. DBDs offer a unique combination of nonequilibrium and quasi-continuous behavior having high electron mean energy with lower heavy particle (neutral, ion) temperature. They produce several chemically active species (electrons, radicals, metastables, and ions) with low gas heating. Because of these characteristics, DBDs are widely used in gas cleaning (from NO_x, SO_x, and VOC), thin-film deposition [1], ozone production, light sources (excimer UV sources) [2], industrial processes of polymer films or fibers to increase the wettability and the adhesion [3], and many other technologies [4]. In addition, DBDs enable various emerging novel applications in biology and medical field [5], [6]. Several interesting medical possibilities have been recently demonstrated by Fridman *et al.* [7].

DBDs are mostly applied at atmospheric pressure, usually in air, and are an uncomplicated way to generate low-temperature atmospheric pressure plasma; however, in most cases, breakdown of an atmospheric pressure gas with the presence of at least one dielectric barrier in the gap results in multistreamer mode of operation with formation of microdischarges [8] and subsequent filaments that are visible to naked eye.

As plasma density in the microdischarges is much higher than that in the surrounding space, these microdischarges can be considered as the only active locations of the whole DBD volume, where all of the energy dissipates and eventually increases the gas temperature at the vicinity and on the surface treated. Energy dissipation is minute but highly localized and can be very important when the surface to be treated is temperature sensitive such as biological materials.

When the plasma is ignited, current passes through these microdischarges which typically have a diameter on the order of 100 μm [9]. However, the dielectric barrier(s) covering the electrodes acts as a capacitor in series with the gas gap, limits the current, and stops the transition to arc. The size, current, and power dissipated within a single microdischarge will determine the associate temperature rise and thermal effects on the treated surface.

In this paper, we investigate the gas temperatures and thermal effects of the DBD using two distinct voltage waveforms in order to improve treatment quality for medical applications. Discharge temperature controllability and the relationship to microdischarge formation are also discussed.

II. Materials and Methods

Microsecond-pulsed and sinusoidal discharges, which are the subject of this paper, have been generated with two electrode configurations. In the first configuration (Fig. 1), the powered electrode is a 25-mm-diameter copper electrode covered with 35-mm-diameter 1-mm-thick clear fused quartz (Technical Glass Products, Painesville, OH) and enclosed in polyetherimide (Ultem). The other electrode was a grounded copper plate placed typically at a 1-mm distance from the quartz surface.

Manuscript received May 5, 2008; revised August 4, 2008. First published November 25, 2008; current version published January 8, 2009. This work was supported in part by DARPA Award W81XWH-05-2-0068.

H. Ayan, D. Staack, and A. A. Fridman are with the Department of Mechanical Engineering and Mechanics, College of Engineering, Drexel University, Philadelphia, PA 19104 USA (e-mail: ha56@drexel.edu; das83@drexel.edu; af55@drexel.edu).

G. Fridman is with the School of Biomedical Engineering, Science, and Health Systems, Drexel University, Philadelphia, PA 19104 USA (e-mail: gf33@drexel.edu).

A. F. Gutsol is with Chevron Energy Technology Company, Richmond, CA 94802 USA (e-mail: alexandergutsol@chevron.com).

V. N. Vasilets is with the Institute for Energy Problems of Chemical Physics, Russian Academy of Sciences, Moscow 142432, Russia (e-mail: vnvasilets@yandex.ru).

G. Friedman is with the Department of Electrical and Computer Engineering, College of Engineering, Drexel University, Philadelphia, PA 19104 USA (e-mail: gary@cbis.ece.drexel.edu).

Color versions of one or more of the figures in this paper are available online at http://ieeexplore.ieee.org.

Digital Object Identifier 10.1109/TPS.2008.2006899

0093-3813/$25.00 © 2008 IEEE

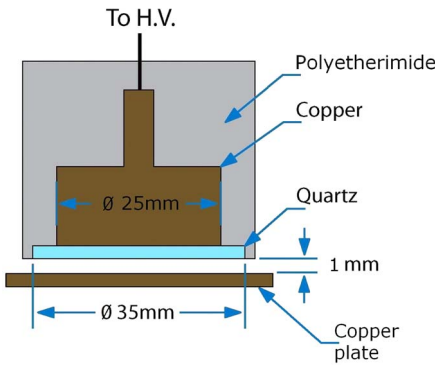


Fig. 1. Cylindrical electrode cross section.

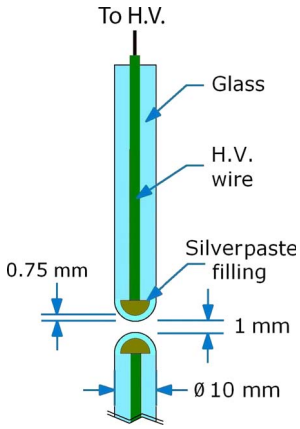


Fig. 2. Glass test tube electrodes.

This configuration was used to compare variations in average temperature with power density for the two voltage waveforms studied. However, in this configuration, the DBD filaments continuously move laterally, and those movements complicate the study of individual filaments. Thus, a second type of electrode configuration was used in order to generate and study single filaments (Fig. 2). This configuration consists of two identical borosilicate glass (Pyrex) test tube (cat.# 60825-902, VWR Scientific, San Francisco, CA) with conductive silver paste (SPI West Chester, PA) filling opposing one another with 1-mm gap spacing. One electrode was powered, and the other was grounded. The thickness of the glass of the test tubes was approximately 0.75 mm, and the glass test tubes' radii of curvature were 5 mm. In this configuration, the filaments are localized at the opposing tips of the electrodes and do not laterally wander. This configuration was used to compare the spatial variations in temperature for the two voltage waveforms studied. The electrode spacing and applied voltages for the two electrode configurations were kept constant so that the systems could be compared, and other than the motion of the filaments in the case of the planar electrodes and significantly lower total current with the rounded electrodes, the systems operated similarly.

Power dissipation in the discharge for each type of DBD in the planar configuration was analyzed by measuring instantaneous current and voltage in the gap (Fig. 4). These measurements were performed using a high-frequency high-voltage probe (#PVM-4, 110 MHz, 1000:1, North Star High Voltage, Marana, AZ) connected in parallel with the discharge and a high-frequency current transformer (#CM-10-L, Ion Physics Corporation, 0.1 V/Amp, 45 MHz bandwidth) around the high-voltage electrode wire. Electrical schematics with voltage and current probes at positions have been published in a previous study [7]. The probe signals were acquired and recorded using a high-speed oscilloscope (500-MHz bandwidth, 5 Gsample/s, TDS5052B Digital Phosphor Oscilloscope, Tektronix, Inc., Richardson, TX). Recorded data were processed using customized MATLAB code which integrates the instantaneous power $(V * I)$ over many cycles to determine an average energy per cycle and average power. Side-view images and typical waveforms of two discharges with planar electrode are given in Figs. 3 and 4, respectively.

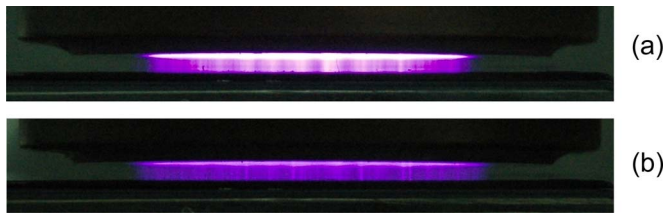


Fig. 3. Images of two discharges with cylindrical electrode (plane-to-plane configuration): (a) Sinusoidal and (b) microsecond-pulsed.

As can be seen in Fig. 4, the current spikes associated with individual microdischarges are characteristically very short in duration, and questions arise in using the measured current to calculate the discharge power. The bandwidth of the current probe and the inverse of the microdischarge duration are comparable, and some loss of information about the actual discharge current may occur. For this reason, the electrical measurements for average power were verified with custom-made calorimetric setup (Fig. 5). This was composed of a peristaltic pump (model # 3386, Control Company, TX), two mercury thermometers (model # 112C, -1–$51\ ^{\circ}$C, $1/10\ ^{\circ}$C div., Palmer Instruments, Inc., NC), a copper chamber, and an insulation casing. Water was pumped with controllable flow rate through the copper tube that surrounds the chamber and encloses the DBD electrodes. One thermometer was placed before the chamber to measure the inlet temperature of the water. A second thermometer was located after the chamber to measure the outlet temperature of the water. The system was insulated to ensure that the only heat loss was to the flowing water.

When the plasma ignited, dissipated energy in the chamber was taken away by copper chamber and copper tube surrounding the chamber and transferred to the running water. Temperature measurements from both thermometers have been recorded every minute throughout the experiments. Since the heat transfer to the water was rather a slow process, it took typically more than 100 min to reach the steady-state conditions. After reaching the steady state, the heat transferred from discharge (thus, the average power dissipation in the discharge gap) could be calculated by using flow rate, water specific heat capacity, and constant water temperature difference between inlet and outlet. It should be noted that the calorimetric and electrical power calculations were comparable, indicating that the bandwidth of the current transformer is at least sufficient for these measurements.

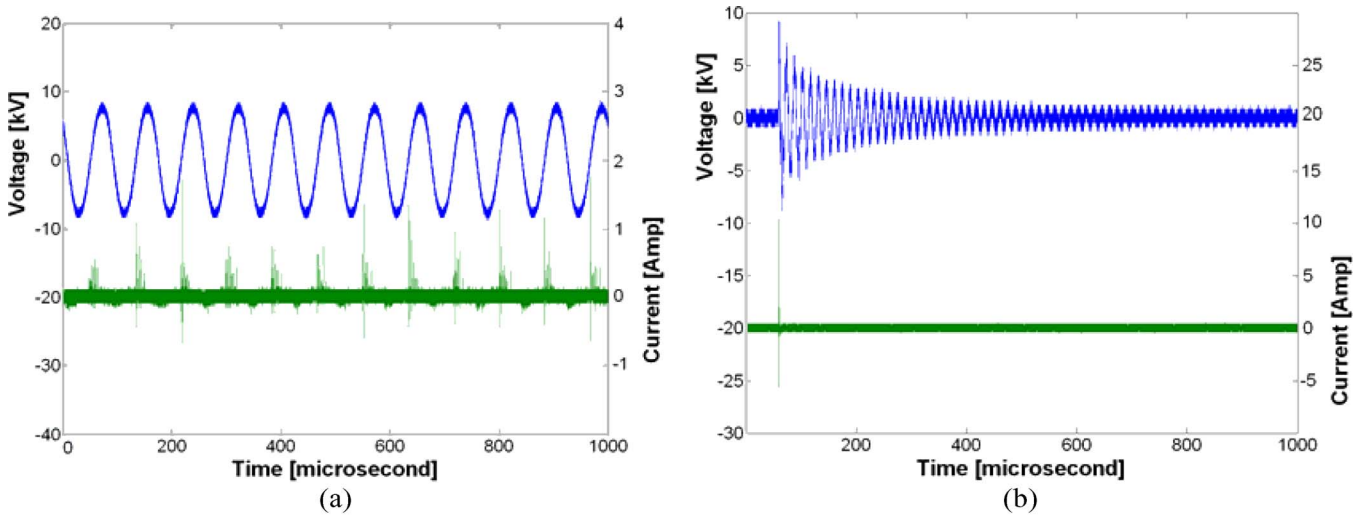


Fig. 4. Typical waveforms of two discharges with cylindrical electrode (plane-to-plane configuration): (a) Sinusoidal and (b) microsecond-pulsed (for both figures: Upper signal is the voltage and lower signal is the current).

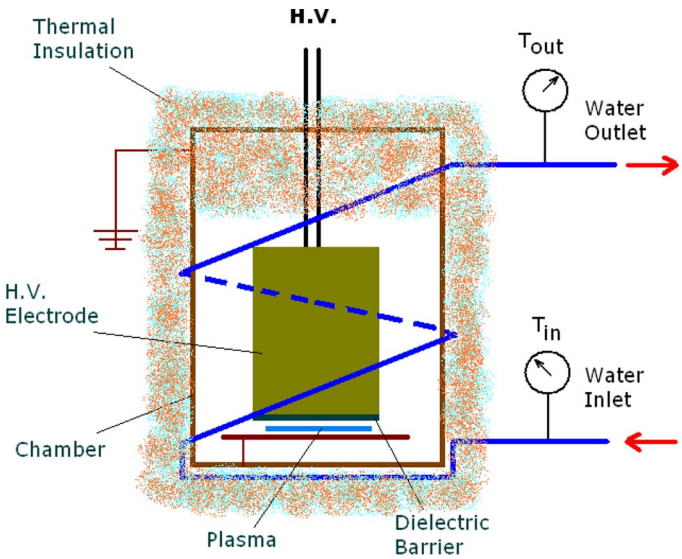


Fig. 5. Schematic of calorimeter setup.

In addition to the voltage, current, and calorimetric measurements, emission spectroscopy was employed to measure the vibrational and rotational temperatures of the DBD volume discharges and single-filament discharges [Fig. 6(a) and (b)] using 375.4- and 380.4-nm vibrational lines and rotational structure at this region of the second positive system of molecular nitrogen, N_2 ($C^3\Pi - B^3\Pi$). Experimental spectrum was compared to simulated spectrum with $T_{\rm vib}$ and $T_{\rm rot}$ determined by the best fit (minimum RMSE) between the modeled and experimental spectra described in detail elsewhere [10]–[14].

In the case of planar electrodes and volume discharge (configuration 1: 25-mm-diameter active area), a fiber-optic bundle (Princeton Instruments-Acton, 10 fibers—200-μm core) was utilized to acquire the emission from the discharge and to transmit it to a spectrometer (Acton Research SpectraPro 500i with Roper Scientific model 7430 CCD camera), and spectra were digitally acquired with approximately 0.6-nm resolution [Fig. 6(a)]. The temperature of the camera was set to -25 °C.

In the case of single-filament discharges (configuration 2), in order to measure spatial distribution of temperature along the filaments, a concave mirror with 5-cm focal length was used to focus the light emitted from the plasma onto the slit of the spectrometer magnifying the image approximately five times similar to as was done in [14] [Fig. 6(b)].

Typical acquisition time for the spectra was 10 s. Background images with the discharge off were subtracted, and a low-pressure mercury lamp was used to determine the slit function of the spectrometer. The entrance slit width was 85 μm when acquiring emission from the discharge and mercury lamp. The ambient room temperature was 22 °C throughout the spectroscopic measurements.

Finally, the measurement of the surface temperature of the grounded electrode in the presence of the discharges was done using a reversible liquid crystal temperature indicator (model 4002B, Accuracy: ± 1 °C, LCR Hallcrest L.L.C., IL). A sheet of the temperature indicator was placed over the grounded copper electrode and acted as the secondary electrode in the discharge. The room temperature was also 22 °C during the surface temperature measurements.

III. Results and Discussion

The features of the two power supplies that have been employed to generate plasma are as follows: 1) microsecond-pulsed power supply that can generate up to 35-kV peak-to-peak voltage with 120 Hz–1 kHz repetition rate and 1.5–5 μs full-width at half-maximum of the voltage pulse, and 2) sinusoidal power supply that can generate up to 35-kV peak-to-peak voltage with 12-kHz frequency. Typical waveforms of two power supplies are given in Fig. 4 where peak-to-peak voltages were 17 kV for sinusoidal and 18 kV for microsecond-pulsed systems.

It should be mentioned that since power supplies used for this study were limited in power capacity, power density ranges did not exactly overlap. Power densities were given as follows: Microsecond-pulsed power supply ranges between 1 and

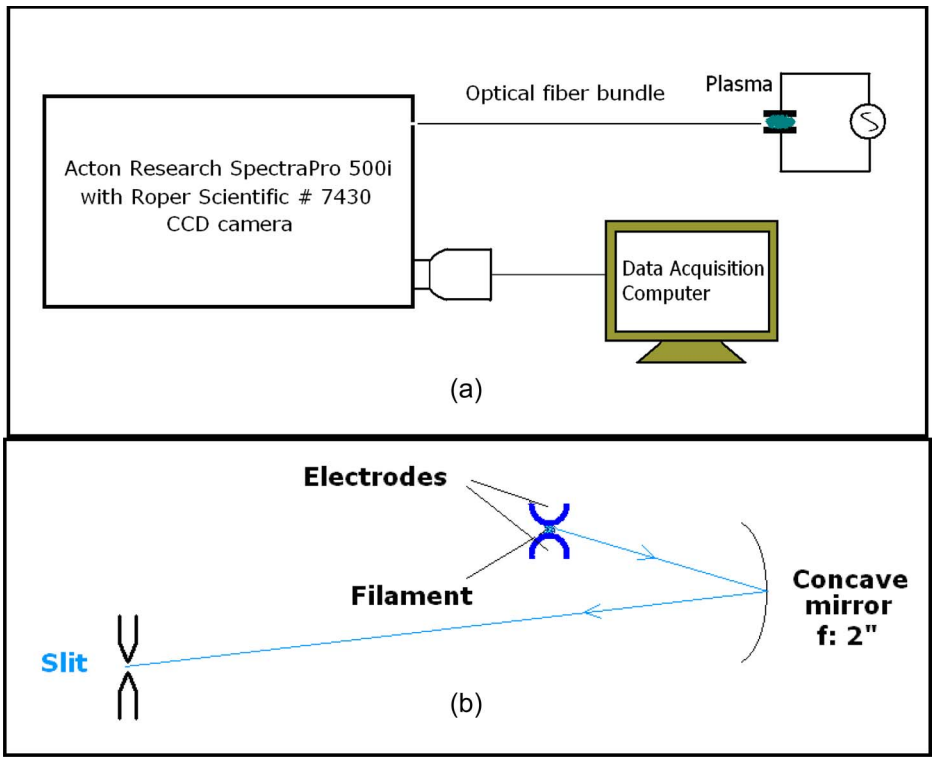


Fig. 6. Spectroscopic measurement setups. (a) For volume discharge and (b) for single filament.

1.5 W/cm^2, and sinusoidal power supply ranges between 1.5 and 3 W/cm^2 (for 25-mm diameter of the active area of the electrode and 1-mm discharge gap).

Oscillograms show that current signals for sinusoidal DBD are multipeak; however, microsecond-pulsed DBD has only one peak with larger amplitude during one period as shown in Fig. 7 [and Fig. 4(a)]. Multiple current peaks for the sinusoidal discharge reflect a typical nonuniform DBD discharge characteristic [8]. On the other hand, the microsecond-pulsed DBD has a single current peak of large magnitude which causes a voltage drop, and this discharge appeared visually less filamentary (filaments are not so bright and stable) than the sinusoidal one. The single large current peak of the pulsed DBD is a result of the faster voltage rise and larger overvoltage.

For the conditions shown in Fig. 7 corresponding to experiments with the plane-to-plane electrode configuration and 1-mm air gap, the power level of sinusoidal DBD was 8.9 W and that of microsecond-pulsed DBD was 7.3 W. Using the 25-mm-diameter active area of the electrode, power densities are calculated to be 1.76 and 1.45 W/cm^2 (or 17.6 and 14.5 W/cm^3), respectively. Electrical measurements were verified by calorimetric power measurements resulting in power values with differences less than 10% of the electrically measured power.

Rotational temperature results for volume discharge (25-mm-diameter active area electrode) are given in Fig. 8, together with the results of surface temperature measurements done with thermochromic liquid crystal temperature indicators for comparison [15].

By these measurements, it is found that the rotational temperatures are between 340 K and 400 K for both types of DBD and that the surface temperatures are 30 K–50 K lower for the same power. The DBD discharges that have been studied here generate nonequilibrium plasmas with rotational temperature essentially equal to the translational (gas) temperature [2], [3], [6], [16]. Since rotational temperature (gas temperature) has been obtained via spectroscopy and the lifetime of upper state of N_2 is very short [17] compared to the shortest voltage pulse duration (microsecond-pulsed DBD), it is likely that the collected light and measured temperature correspond to the plasma state during the time of the microdischarge. In contrast to the spectroscopy which measures the temperature during the time of the microdischarges, the surface temperature measurements indicate a time-averaged temperature. The measured volume and surface temperatures are related since the temperature of the liquid crystal indicators on the grounded electrode surface was reached because of the average heat transferred to it, which is determined by the mean temperature of the volume. A near-linear increase in temperature, both volume and surface, with average power density, as is shown in Fig. 8, is observed as might be expected. Moreover, the two distinct types of voltage waveforms seem to fit to the same slope (although no overlap is seen within their respective operating ranges due to power supply limitations). This demonstrates that the power–temperature relation is largely independent of voltage waveform shape for the power range studied here. Thus, although sterilization effects may be different for different discharges, i.e., dependent on several physical and chemical factors, it appears that gas temperature depends only on average power. From the perspective treatment quality in terms of comfort to the patient, the average power is one of the most important parameters.

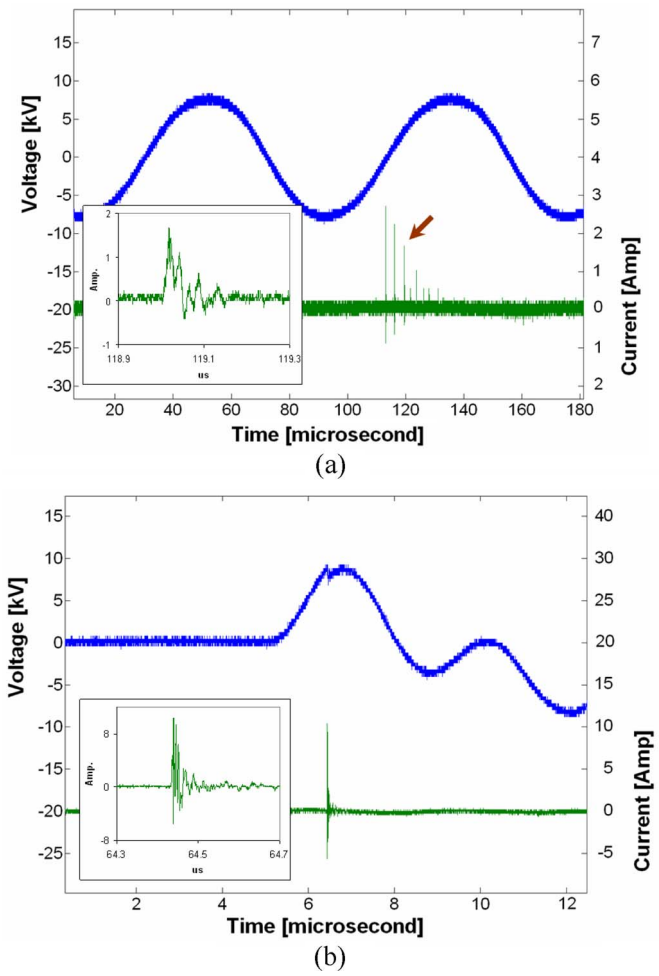


Fig. 7. Comparison of current signal between (a) sinusoidal and (b) microsecond-pulsed DBDs using the plane-to-plane configuration (for both figures: The upper signal is the voltage and the lower signal is the current). The insets at lower-left corner illustrate the current pulses with shorter time scale.

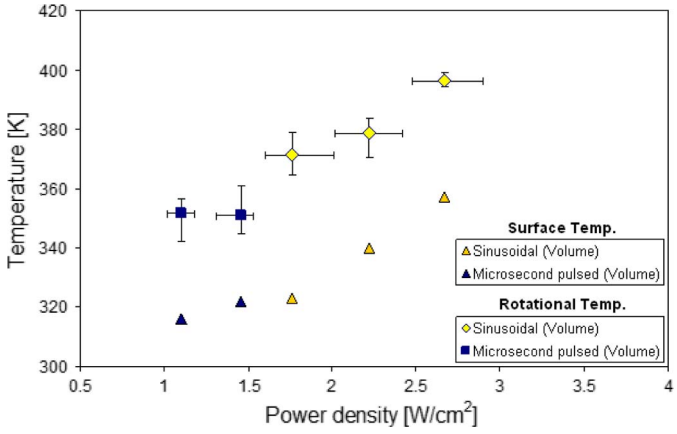


Fig. 8. Rotational and surface temperatures as function of average power density for the sinusoidal power supply and the microsecond-pulsed power supply both using the plane-to-plane electrode configuration (volume).

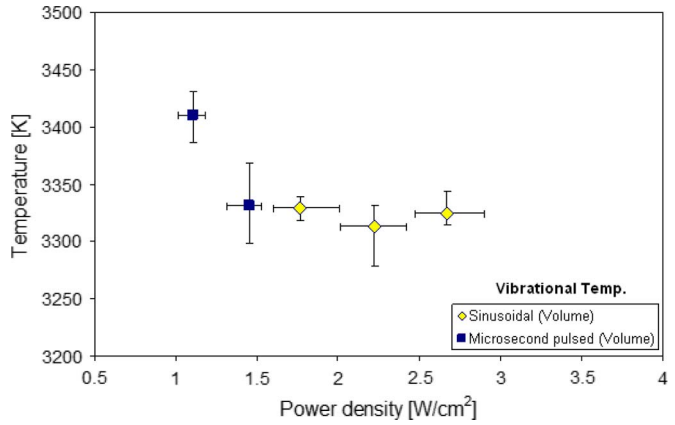


Fig. 9. Vibrational temperatures as function of average power density.

The rotational and vibrational temperatures given in Figs. 8 and 9 are averages of three measurements for the same conditions, and the error bars shown are based upon the statistics of these three measurements. In Fig. 9, vibrational temperatures are given as a function of average power density. Even though it looks like there exists a trend of decreasing vibrational temperature at higher power levels, this is not really clear because of the relatively low sensitivity of the calculation method to the vibrational temperature; thus, we can consider all values to be roughly the same (3300 K–3400 K). Nonetheless, an increase in vibrational temperature with decreasing rotational temperature has been observed before and is not unexpected as the rates of vibrational-to-translational energy transfer decrease with decreasing translational temperature [13]. These results indicate that in addition to the desirable lower gas temperatures for microsecond-pulsed discharges, the vibrational energy (which enhances chemistry and that probably leads to sterilization) is also desirably maintained or even higher for the microsecond-pulsed discharges.

In addition to the volume discharge temperatures, spatial temperature distribution along a single filament has also been measured in order to investigate effects of energy dissipation in the volume onto near-surface locations. Double glass test tube electrode configuration with 1-mm distance between electrodes was used to obtain single filament. Temperatures for the two different types of DBD filaments have been measured over 20 equally divided intervals (at 21 cross sections) along the axial direction. In Fig. 10, cross-sectional locations along the filament axis are shown with transversely drawn lines on the filament images that have been captured with CCD camera at image mode. The radial thickness of the microsecond-pulsed DBD is clearly seen to be thinner than that of the sinusoidal DBD. This may be due to the fact that the volumetric "memory" effect [9] is stronger for sinusoidal DBD, which has a much higher current pulsing frequency, and therefore, each streamer has better marked "road" that is formed by the diffuse decay of the previous streamer.

Results of temperature measurements at the aforementioned positions, along the discharge channel, are given in Fig. 11. These measurements do not reveal any significant difference at rotational and vibrational temperatures along the discharge channel (except possibly very near the electrodes). Rotational temperature distributions are uniform along filament for both types of discharges; thus, power appears to dissipate more or less evenly.

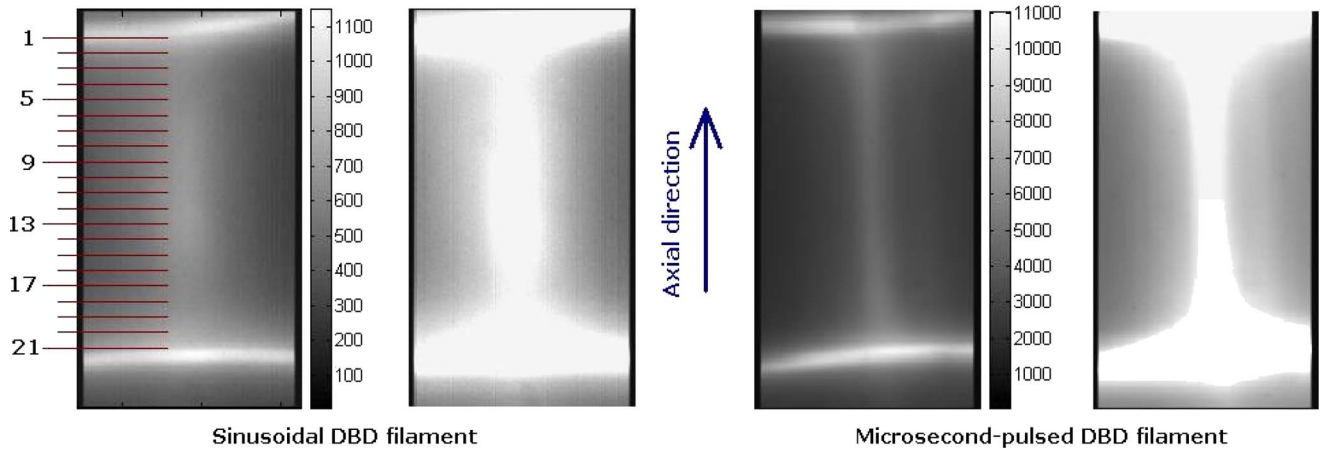


Fig. 10. Images of two types of DBDs with locations of the 21 cross sections (1-mm gap). Exposure time of sinusoidal DBD is 50 ms (600 cycles) and microsecond-pulsed DBD is 1 s (1000 cycles) (left images of each type of discharges are actual images, and right ones of each type of discharges are contrast enhanced).

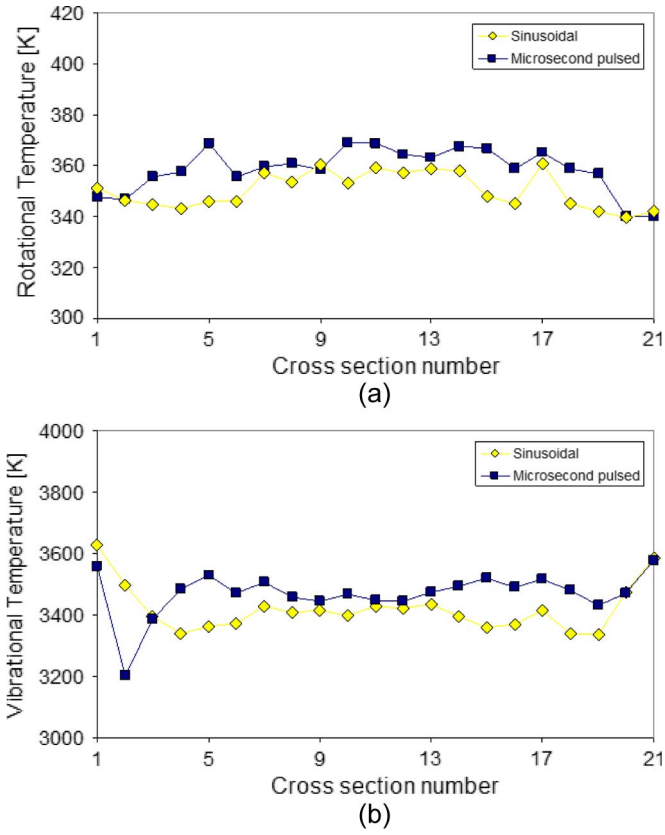


Fig. 11. (a) Rotational and (b) vibrational temperature distribution along the discharge channel.

Along the center axis, emission intensity (of the region of interest of the spectrum) from the single filament is minimal in the middle, and it increases toward the electrode surfaces, roughly doubles for both types of discharges studied here. However, as shown in Fig. 11, an increase in emission intensity does not mean that the temperature is higher. Moreover, a slight increase of the light intensity at the electrodes might be due to inevitable reflection from the glass test tube surfaces. In summary, Fig. 11(a) and (b) indicates that the rotational and vibrational temperatures can be considered constant along the channel. In general, vibrational temperatures are one order of magnitude higher than rotational temperatures, and this indicates the nonequilibrium nature of the discharge.

IV. Conclusion

Both DBD systems have been analyzed visually, electrically, and spectroscopically. Single-filament measurements showed that there is no significant change in gas temperature along the channel. Volume discharge measurements demonstrated that microdischarges within the volume for different types of discharges have the same gas temperature for the same power. In general, gas (translational) temperature is growing with power within the ranges of 1.5–3 W/cm^2 (7.5–15 W) for sinusoidal and 1–1.5 W/cm^2 (5–7.5 W) for microsecond-pulsed DBDs. The temperature of the microsecond-pulsed discharge tends to be lower than that for the sinusoidal ac discharge, although this effect is mainly related to the lower power. The voltage pulse duration (few microseconds) is still not short enough to create significant difference (for example, filament-free discharge). Employing even shorter pulsed driving waveform is possibly one of the ways to maintain high vibrational temperature while lowering the rotational temperature of discharge. Shortening pulse durations down to less than microsecond would restrict the evolution of streamers in time and avoid multifilamentary structure of plasma [8], [9]. For pulses longer than microsecond, in general, using small-size plasma (in axial and/or radial dimensions) or using small-gap DBD configurations would result in discharges with lower power levels, keeping temperature low.

When working with DBDs for medical applications involving living tissue, a question arises about temperature of the process. For better quality and controllable treatment of living tissue, a nonheating discharge is required. Considering, for instance, sterilization of the living tissue, the effects may be different for different discharges. While sterilization is dependent on several physical and chemical factors such as composition of gas and distribution of many microdischarges, the gas temperature depends only on average power, as shown

in this paper. Thus, average power is not the only parameter responsible from the perspective of sterilization but is one of the parameters which define treatment quality in terms of comfort to the patient. There exist regimes with lower power that only have the effect of interest, i.e., sterilization, etc., without any trace of burning. However, if desired, one can obtain regimes with increasing the power that burns. Although surface temperature is less than microdischarge temperature, there is a direct correlation. That is why increasing the average temperature will result in increase at surface temperature of the treated tissue (or material).

REFERENCES

[1] J. M. Williamson, D. D. Trump, P. Bletzinger, and B. N. Ganguly, "Comparison of high-voltage ac and pulsed operation of a surface dielectric barrier discharge," *J. Phys. D, Appl. Phys.*, vol. 39, no. 20, pp. 4400–4406, Oct. 2006.

[2] O. Motret, C. Hilbert, S. Pellerin, and J. M. Pouvesle, "Rotational temperature measurements in atmospheric pulsed dielectric barrier discharge—Gas temperature and molecular fraction effects," *J. Phys. D, Appl. Phys.*, vol. 33, no. 12, pp. 1493–1498, Jun. 2000.

[3] F. Massines, R. Messaoudi, and C. Mayoux, "Comparison between air filamentary and helium glow dielectric barrier discharges for the polypropylene surface treatment," *Plasmas Polym.*, vol. 3, no. 1, pp. 43–59, Mar. 1998.

[4] A. Fridman, A. Chirokov, and A. Gutsol, "TOPICAL REVIEW—Nonthermal atmospheric pressure discharges," *J. Phys. D, Appl. Phys.*, vol. 38, no. 2, pp. R1–R24, Jan. 2005.

[5] M. Laroussi, I. Alexeff, and W. L. Kang, "Biological decontamination by nonthermal plasmas," *IEEE Trans. Plasma Sci.*, vol. 28, no. 1, pp. 184–188, Feb. 2000.

[6] E. Stoffels, A. J. Flikweert, W. W. Stoffels, and G. M. W. Kroesen, "Plasma needle: A non-destructive atmospheric plasma source for fine surface treatment of (bio)materials," *Plasma Sources Sci. Technol.*, vol. 11, no. 4, pp. 383–388, Nov. 2002.

[7] G. Fridman, M. Peddinghaus, H. Ayan, A. Fridman, M. Balasubramanian, A. Gutsol, A. Brooks, and G. Friedman, "Blood coagulation and living tissue sterilization by floating-electrode dielectric barrier discharge in air," *Plasma Chem. Plasma Process.*, vol. 26, no. 4, pp. 425–442, Aug. 2006.

[8] U. Kogelschatz, "Dielectric-barrier discharges: Their history, discharge physics, and industrial applications," *Plasma Chem. Plasma Process.*, vol. 23, no. 1, pp. 1–46, Mar. 2003.

[9] U. Kogelschatz, "Filamentary, patterned, and diffuse barrier discharges," *IEEE Trans. Plasma Sci.*, vol. 30, no. 4, pp. 1400–1408, Aug. 2002.

[10] A. P. Yalin *et al.*, "Spatial profiles of N_2^+ concentration in an atmospheric pressure nitrogen glow discharge," *Plasma Sources Sci. Technol.*, vol. 11, no. 3, pp. 248–253, Mar. 2002.

[11] C. O. Laux *et al.*, "Optical diagnostics of atmospheric pressure air plasmas," *Plasma Sources Sci. Technol.*, vol. 12, no. 2, pp. 125–138, May 2003.

[12] D. Packan *et al.*, "Measurement and Modeling of OH, NO, and CO_2 infrared radiation at 3400 K," *J. Thermophys. Heat Transf.*, vol. 17, no. 4, pp. 450–456, 2003.

[13] D. Staack, B. Farouk, A. F. Gutsol, and A. A. Fridman, "Spectroscopic studies and rotational and vibrational temperature measurements of atmospheric pressure normal glow plasma discharges in air," *Plasma Sources Sci. Technol.*, vol. 15, no. 4, pp. 818–827, Nov. 2006.

[14] D. Staack, B. Farouk, A. F. Gutsol, and A. A. Fridman, "Spatially resolved temperature measurements of atmospheric-pressure normal glow microplasmas in air," *IEEE Trans. Plasma Sci.*, vol. 35, no. 5, pp. 1448–1455, Oct. 2007.

[15] J. Goree, B. Liu, D. Drake, and E. Stoffels, "Killing of *S. mutans* bacteria using a plasma needle at atmospheric pressure," *IEEE Trans. Plasma Sci.*, vol. 34, no. 4, pp. 1317–1324, Aug. 2006.

[16] T. Nozaki, Y. Miyazaki, Y. Unno, and K. Okazaki, "Energy distribution and heat transfer mechanisms in atmospheric pressure non-equilibrium plasmas," *J. Phys. D, Appl. Phys.*, vol. 34, no. 23, pp. 3383–3390, Dec. 2001.

[17] A. Chelouah, E. Marode, G. Hartmann, and S. Achat, "A new method for temperature evaluation in a nitrogen discharge," *J. Phys. D, Appl. Phys.*, vol. 27, no. 5, pp. 940–945, May 1994.



Halim Ayan was born in Izmir, Turkey, in 1979. He received the B.S. degree in mechanical engineering from Ege University, Izmir, Turkey, in 2001. He is currently working toward the Ph.D. degree in the Department of Mechanical Engineering and Mechanics, College of Engineering. Drexel University, Philadelphia, PA.

His research focuses on discharge physics and uniformity of the atmospheric pressure dielectric barrier discharge at the Drexel Plasma Institute. His research interests include applications of nonthermal plasmas for medical applications.



Gregory Fridman received the B.S. degree in mathematics, statistics, and computer science from the University of Illinois, Chicago, in 2002, and the M.S. degree in biomedical science from Drexel University, Philadelphia, PA. He is currently working toward the Ph.D. degree at the School of Biomedical Engineering, Science, and Health Systems, Drexel University.

His research interests include the use of nonequilibrium plasma for processing of biomaterials; polymer treatment and surface modification for wettability and biocompatibility; applications of nonequilibrium discharges in medicine and biology; characterization of physical, biochemical, and mechanical properties of the treated material; plasma characterization; and plasma power supply design and development.



David Staack was born in New York, NY, in 1977. He received the B.S. and M.S. degrees in aerospace engineering from the University of Virginia, Charlottesville, in 2000. Since 2004, he has been working toward the Ph.D. degree in mechanical engineering in the Department of Mechanical Engineering and Mechanics, Drexel University, Philadelphia, PA.

At the University of Virginia, his thesis research was on developing and using LIF techniques for the diagnostics of interacting rarified and continuum flows. From 2000 to 2004, he was with the Princeton Plasma Physics Laboratory, Princeton University, Princeton, NJ, where he was studying the effects of plasma surface interactions on the performance of Hall Thruster rocket engines and developing plasma diagnostics. At the A. J. Drexel Plasma Institute, his research has focused on the characterization of atmospheric pressure nonthermal plasmas and the use of such plasmas for plasma-enhanced chemical vapor deposition, biomedical applications, and fuel reforming. As of January 2009, he will be an Assistant Professor with the Mechanical Engineering Department, Texas A&M University, College Station, TX. His research interests include plasma engineering applications of low-temperature plasmas at various pressures and in various media, and plasma discharge and flow diagnostics.



Alexander F. Gutsol was born in Magnitogorsk, Russia, in 1958. He received the B.S. and M.S. degrees in physics and engineering and the Ph.D. degree in physics and mathematics from the Moscow Institute of Physics and Technology (working for the Kurchatov Institute of Atomic Energy), Moscow, Russia, and the D.Sc. degree in mechanical engineering from the Baykov Institute of Metallurgy and Material Science, Moscow.

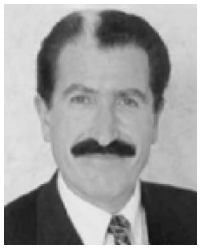
From 1985 to 2000, he was with the Institute of Chemistry and Technology of Rare Elements and Minerals, Kola Science Center, Russian Academy of Sciences, Apatity, Russia. As a Visiting Researcher, he worked in Israel in 1996, Norway in 1997, Netherlands in 1998, and Finland from 1998 to 2000. From 2000 to 2002, he was with the University of Illinois, Chicago. From 2002 to 2008, he was with Drexel University, Philadelphia, PA, where he was a Research Professor with the Department of Mechanical Engineering and Mechanics, College of Engineering, and an Associate Director of the Drexel Plasma Institute. He is currently with Chevron Energy Technology Company, Richmond, CA. During his scientific carrier, he was involved in electrical-discharge physics, chemistry and engineering, fluid dynamics, chemistry and technology of rare metals, and powder metallurgy.



Victor N. Vasilets was born in Murmansk, Russia, in 1953. He received the B.S. and M.S. degrees in physics and engineering and the Ph.D. degree in physics and mathematics from the Moscow Institute of Physics and Technology, Moscow, Russia, in 1976 and 1979, respectively, and the D.Sc. degree in chemistry from the N. N. Semenov Institute of Chemical Physics, Russian Academy of Sciences, Moscow, in 2005.

He was a Research Scientist in 1979, a Senior Research Scientist in 1987, and a Principal Research Scientist in 2000 with the N. N. Semenov Institute of Chemical Physics. He was invited as a Visiting Professor with the Center of Biomaterials, Kyoto University, Kyoto, Japan (in 1996); the Institute of Polymer Research, Dresden, Germany (from 1998 to 2000); and the Plasma Physics Laboratory, University of Saskatchewan, Saskatoon, SK, Canada (from 2002 to 2005). During 2005–2007, he was with the Department of Mechanical Engineering and Mechanics, Drexel University, Philadelphia, PA, as a Research Professor. He is currently the Principal Research Scientist with the Institute for Energy Problems of Chemical Physics, Russian Academy of Sciences. He has authored or coauthored three book chapters and more than 100 papers. His current research interests focus on using gas discharge plasma and vacuum ultraviolet for sterilization, wound treatment, and biological functionalization of medical polymers.

Dr. Vasilets is a member of the International Advisory Board of the journal *Plasma Processes and Polymers*.



Alexander A. Fridman received the B.S., M.S., and Ph.D. degrees in physics and mathematics from the Moscow Institute of Physics and Technology, Moscow, Russia, in 1976 and 1979, respectively, and the D.Sc. degree in mathematics from the Kurchatov Institute of Atomic Energy, Moscow, in 1987.

He is currently the Nyheim Chair Professor with the Department of Mechanical Engineering and Mechanics, College of Engineering, Drexel University, Philadelphia, PA, and the Director of the Drexel Plasma Institute, where he works on plasma approaches to material treatment, fuel conversion, and environmental control. He has more than 30 years of plasma research experience in national laboratories and universities of Russia, France, and USA. He has authored or coauthored five books and more than 350 papers.

Prof. Fridman was a recipient of numerous awards, including the Stanley Kaplan Distinguished Professorship in Chemical Kinetics and Energy Systems, the George Soros Distinguished Professorship in Physics, and the State Prize of the U.S.S.R. for the discovery of selective stimulation of chemical processes in nonthermal plasma.



Gary Friedman received the Ph.D. degree in electrical engineering, with specialization in electrophysics, from the University of Maryland, College Park.

From 1989 to 2001, he was a Faculty Member with the Department of Electrical Engineering and Computer Science, University of Illinois, Chicago. Since September 2001, he has been with the Department of Electrical and Computer Engineering, College of Engineering, Drexel University, Philadelphia, PA, as a Full Professor, where he directs activities of the Magnetic Microsystems Laboratory and is a member of the Drexel Plasma Institute. His current research interests include magnetically programmed self-assembly, magnetic separation in biotechnology, magnetically targeted drug delivery, magnetic tweezing as a tool for investigation of living cells, design and fabrication of microcoils for nuclear magnetic resonance spectroscopy, and imaging of live cells and modeling of hysteresis in magnetic systems and complex networks. He is also interested in the development of cold atmospheric pressure plasma technology for applications in biotechnology and medicine.